Polyhedron 28 (2009) 1379–1385

Contents lists available at ScienceDirect

Polyhedron

journal homepage: www.elsevier.com/locate/poly

Bis(piperazin-1-ium) tetrasulfidometalates: Solid state synthesis, thermal studies and structural characterization ☆

Bikshandarkoil R. Srinivasan [a,*], Ashish R. Naik [a], Martha Poisot [b,1], Christian Näther [b], Wolfgang Bensch [b]

[a] Department of Chemistry, Goa University, Goa 403 206, India
[b] Institut für Anorganische Chemie, Christian-Albrechts-Universität Kiel, Olshausenstraße 40, D-24098 Kiel, Germany

ARTICLE INFO

Article history:
Received 13 January 2009
Accepted 24 February 2009
Available online 9 March 2009

Keywords:
Tetrasulfidometalate
Piperazin-1-ium
N–H···N interactions
Endothermic
Piperazinediium

ABSTRACT

The organic tetrasulfidometalates $(pipH)_2[MS_4]$ (pipH = piperazin-1-ium; M = W **1**; M = Mo **2**) were prepared by a mechanical grinding of solid $(NH_4)_2[MS_4]$ (M = Mo or W) with the cyclic diamine piperazine (pip). Compounds **1** and **2** which contain the monoprotonated cation of piperazine were characterized by elemental analysis, infrared, Raman and UV–Vis spectra and their structures were determined. The title compounds decompose endothermically to carbon containing metal disulfide residues. Both compounds are isostructural and crystallize in the centrosymmetric triclinic space group $P\bar{1}$. The structures of both compounds consist of two crystallographically independent piperazin-1-ium cations and a tetrasulfidometalate dianion, with all atoms situated in general positions. An intramolecular N–H···N interaction links the organic cations into pairs and the pairs thus formed extend into a one-dimensional chain of cations with the aid of an intermolecular N–H···N bond. The $[MS_4]^{2-}$ anions are linked to the chains of piperazin-1-ium cations via N–H···S and C–H···S interactions. A comparative study of the spectral, structural and thermal properties of the title compounds with those of the previously reported $(pipH_2)[MS_4]$ ($pipH_2$ = piperazinediium) compounds containing the $(pipH_2)^{2+}$ dication is described.

1. Introduction

The chemistry of the group VI tetrasulfidometalates $[MS_4]^{2-}$ (M = Mo, W) is an area of intense research investigations as evidenced by several reports in the literature [1–10]. The tetrahedral $[MS_4]^{2-}$ dianions are well known for their use as starting materials for the preparation of a variety of metal–sulfur compounds including catalytically important group VI metal sulfide materials [6–13]. Recent work by the Jakobsen group on the use of $(NH_4)_2[MS_4]$ for advancements in natural abundance solid state ^{33}S MAS NMR spectroscopy [14–16] has generated renewed interest in the chemistry of these compounds and the reinvestigation of $(PPh_4)_2[M'(WS_4)_2]$ (M′ = Co, Ni, Zn) materials [17] indicates that a rich structural chemistry still remains to be developed. During the course of our studies of the sulfur compounds of Mo and W [18–23] we have developed a convenient method for the facile synthesis of tetrahedral $[MS_4]^{2-}$ compounds stabilized by organic ammonium cations [22–27]. Our method involves the direct reaction of $(NH_4)_2[MS_4]$ with an organic amine and this work has resulted in the structural characterization of several new compounds. Prior to our work, the reactions of tetraalkylammonium hydroxide with $[MS_4]^{2-}$ or tetraalkylammonium halide with $[MS_4]^{2-}$ in the presence of NaOH were shown to result in the formation of organic soluble $[R_4N]_2[MS_4]$ (R = alkyl) compounds [28,29].

The organic $[MS_4]^{2-}$ compounds reported by us and others [22–50] exhibit several weak H-bonding interactions between the $[MS_4]^{2-}$ anion and the organic ammonium cation. These interactions (especially N–H···S) can be tuned by varying the steric bulk as well as the number of potential donor H atoms on the amine, with the organic cations functioning as handles to distort the $[MS_4]^{2-}$ tetrahedron, as evidenced by the observation of distinct Mo–S or W–S distances in several compounds. In earlier reports we have shown that the compounds $(pipH_2)[MS_4]$ ($pipH_2$ = piperazinediium) prepared by an aqueous reaction of $(NH_4)_2[MS_4]$ with the cyclic diamine piperazine (pip) exhibit one of the longest W–S (2.2147(7) Å) or Mo–S (2.2114(8) Å) distances [26,27]. Further the $(pipH_2)[MS_4]$ compounds thermally decompose resulting in the formation of amorphous metal sulfide residues containing considerable amounts of C. We have also observed that some amines like cyclohexane-1,2-diamine (1,2-cn), diethylenetriamine (dien) and tris(2-aminoethylamine) (tren) form $[MS_4]^{2-}$ compounds charge balanced by partially protonated organic ammonium cations like $(1,2\text{-cnH})^+$ $(dienH_2)^{2+}$ and $(trenH_2)^{2+}$ [34–38]. The cyclic diamine pip can function as a monoprotonated piperazin-1-ium cation $(pipH)^+$ or as a diprotonated $(pipH_2)^{2+}$ cation (Scheme 1). Hence it was of interest to investigate the effect of the mono cation

☆ Dedicated to Dr. Herbert Pausch on the occasion of his 65th birthday.

* Corresponding author. Tel.: +91 832 6519316; fax: +91 832 2451184.
E-mail addresses: srini@unigoa.ac.in, brsrinivasan@gmail.com (B.R. Srinivasan).
[1] Present address: Universidad del Papaloapan, Circuito Central 200, Parque Industrial, Tuxtepec 68301, Mexico.

0277-5387/$ - see front matter © 2009 Elsevier Ltd. All rights reserved.
doi:10.1016/j.poly.2009.02.034

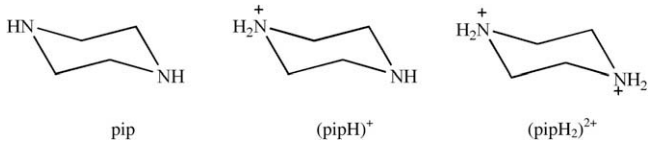

Scheme 1.

$(pipH)^+$ on the metal–sulfur distances as well as the thermal decomposition products. It is interesting to note that the synthesis of such a $[MS_4]^{2-}$ compound containing the $(pipH)^+$ cation could be accomplished by a mechanical grinding of the reactants. The results of these investigations are described in this paper.

2. Experimental

2.1. Materials and methods

All the chemicals used in this study were of reagent grade and were used as received. The ammonium salts of the group VI tetrasulfidometalates were prepared by a published procedure [28]. Far-IR spectra (range 80–500 cm^{-1}) were recorded using a Bruker IFS 66 infrared spectrometer in pressed polyethylene disks. MIR spectra were recorded in a KBr matrix using a Shimadzu (IR Prestige-21) FT-IR spectrometer and a ATI Mattson Genesis infrared spectrometer in the range 4000–400 cm^{-1}. Raman spectra were recorded in the region 100–3500 cm^{-1} on a Bruker FRA 106 Fourier Transform Raman spectrometer. UV–Vis spectra were recorded on a Shimadzu UV-2450 double beam spectrophotometer using matched quartz cells. TG-DTA measurements were performed in nitrogen atmosphere, in Al_2O_3 crucibles on a STA-409CD simultaneous thermal analyzer from Netzsch. A heating rate of 4 K min^{-1} was employed for all measurements.

2.2. Preparation of $(pipH)_2[MS_4]$ (M = W **1**; M = Mo **2**)

Anhydrous piperazine (1.72 g, 10 mmol) was mixed with $(NH_4)_2[WS_4]$ (0.696 g, 2 mmol) and the solid mixture was mechanically ground in a mortar with a pestle for ~5 min. The resulting fine powder was dissolved in water (~10 mL) and briefly warmed on a water bath to expel traces of ammonia. The reaction mixture was filtered and the yellow filtrate was left aside for crystallization to obtain yellow needles. The crystalline product was isolated by filtration, washed with 2-propanol, followed by diethyl ether and air dried to yield 0.5 g of compound **1** in 51% yield. The use of freshly prepared $(NH_4)_2[MoS_4]$ (0.520 g, 2 mmol) instead of $(NH_4)_2[WS_4]$ in the above reaction afforded compound **2** as red needles in 60% yield. The needles of **1** and **2** thus obtained are suitable for X-ray structure determination.

Anal. Calc. for $(C_4H_{11}N_2)_2WS_4$ (**1**): C, 19.75; H, 4.56; N, 11.52; S, 26.37; WS_4, 64.17. Found: C, 19.79; H, 4.56; N, 11.55; S, 27.26; WS_4, 64.31%.

IR data (cm^{-1}): 3227 $\upsilon_{(N-H)free}$, 3022, 2972, $\upsilon_{(N-H)}$ 2800, 2708, 2582, 2528, 2420, 2388, 2183, 1597, 1462, 1391, 1365, 1323, 1307, 1217, 1165, 1107, 1078, 1051, 1001, 960, 891, 866, 841, 814, 613, 588, 481 (υ_1), 465 (υ_3), 445, 413, 397.

Raman data (cm^{-1}): 3229, 2997, 2964, 2948, 2907, 1437, 1330, 1018, 815, 481 (υ_1), 462 (υ_3), 442, 195, 178 (υ_2, υ_4).

UV–Vis data in nm (mol^{-1} L cm^{-1}): 393 (17360), 277 (25850).

Anal. Calc. for $(C_4H_{11}N_2)_2MoS_4$ (**2**): C, 24.11; H, 5.56; N, 14.06; S, 32.19; MoS_4, 56.26. Found: C, 23.95; H, 5.63; N, 14.02; S, 32.55; MoS_4, 56.12%.

IR data (cm^{-1}): 3223 $\upsilon_{(N-H)free}$, 3022, 2972 $\upsilon_{(N-H)}$, 2798, 2706, 2582, 2528, 2420, 2388, 2181, 1593, 1462, 1445, 1390, 1366, 1323, 1306, 1217, 1165, 1107, 1078, 1051, 1001, 961, 891, 864, 840, 814, 613, 590, 482, 472, 456, 450, 415, 396.

Table 1
Crystal data and structure refinement for compounds **1** and **2**.

Empirical formula	$(C_4H_{11}N_2)_2[WS_4]$ **1**	$(C_4H_{11}N_2)_2[MoS_4]$ **2**
Formula weight (g mol^{-1})	486.39	398.48
Temperature (K)	220(2)	293(2)
Wavelength (A)	0.71073	0.71073
Crystal system	triclinic	triclinic
Space group	$P\bar{1}$	$P\bar{1}$
Unit cell dimensions (Å, °)	a = 8.2524(7)	a = 8.2760(10)
	b = 9.7528(8)	b = 9.7570(10)
	c = 11.5897 (9)	c = 11.604 (2)
	α = 93.068(10)	α = 92.960(10)
	β = 101.772(10)	β = 101.860(10)
	γ = 115.111(9)	γ = 115.180(10)
Volume (Å^3)	816.47(12)	819.57(19)
Z	2	2
D_{calc} (mg/m^3)	1.978	1.615
Absorption coefficient (mm^{-1})	7.572	1.296
F(000)	472	408
Crystal size (mm^3)	0.2 × 0.18 × 0.17	0.15 × 0.14 × 0.14
θ range for data collection (°)	2.34–28.01	1.82–27.02
Index ranges	$-10 \leqslant h \leqslant 10$,	$0 \leqslant h \leqslant 10$,
	$-12 \leqslant k \leqslant 12$,	$-12 \leqslant k \leqslant 11$,
	$-15 \leqslant l \leqslant 15$	$-14 \leqslant l \leqslant 14$
Reflections collected	8498	3844
Independent reflections (R_{int})	3885 (0.0849)	3591 (0.0291)
Reflections with [$I > 2\sigma(I)$]	3588	2984
Completeness to θ (%)	98.6	99.8
Refinement method	full-matrix least-squares on F^2	full-matrix least-squares on F^2
Data/restraints/parameters	3885/0/155	3591/0/155
Goodness-of-fit on F^2	1.016	1.033
Final R indices [$I > 2\sigma(I)$]	R_1 = 0.0355,	R_1 = 0.0243,
	wR_2 = 0.0892	wR_2 = 0.0595
R indices (all data)	R_1 = 0.0383,	R_1 = 0.0394,
	wR_2 = 0.0905	wR_2 = 0.0626
Extinction coefficient	0.0143(10)	0.0169(12)
Largest difference in peak and hole (e Å^{-3})	2.614 and −3.500	0.349 and −0.527

Raman data (cm^{-1}): 3225, 2974, 2963, 2946, 2924, 2906, 1436, 1329, 1022, 815, 483, 471 (υ_3), 456, 448 (υ_1), 177 (υ_2, υ_4).

UV–Vis data in nm (mol^{-1} L cm^{-1}): 468 (8190), 316 (12320), 241 (19190).

2.3. X-ray crystal structure determination

Intensity data were collected on a STOE-Image Plate diffraction System (IPDS 1) for compound **1** and on an AED-2 four-circle diffractometer for compound **2** using graphite-monochromated Mo Kα radiation. The structures were solved with direct methods using SHELXS-97 [51] and refinement was done against F^2 using SHELXL-97 [51]. All non-hydrogen atoms were refined anisotropically. The C–H hydrogen atoms were positioned with idealized geometry and refined using a riding model. The N–H hydrogen atoms were located in the difference map, their bond lengths set to ideal values and afterwards they were refined isotropic using a riding model. The technical details of data acquisition and some selected refinement results are summarized in Table 1.

3. Results and discussion

3.1. Synthesis and spectroscopy

In earlier work we have shown that the reaction of an aqueous solution of $(NH_4)_2[MS_4]$ with piperazine (pip) in a 1:1 ratio results in the formation of $(pipH_2)[MS_4]$ compounds [26,27] containing the diprotonated cation of pip namely $(pipH_2)^{2+}$ (Eq. (1)). All our efforts to prepare $(pipH)_2[MS_4]$ compounds, which contain a monoprotonated cation of pip by the reaction of aqueous solutions

of $(NH_4)_2[MS_4]$ with pip in a 1:2 mole ratio, or use of an excess of pip or alternatively the aqueous reaction of $(pipH_2)[MS_4]$ with pip always resulted in the isolation of products containing either the known $(pipH_2)[MS_4]$ compound or a mixture of products containing $(pipH_2)[MS_4]$ as the major product. As different solution methods of synthesis did not result in the formation of a $[MS_4]^{2-}$ compound containing monoprotonated pip, the reaction of $(NH_4)_2[MS_4]$ with pip was investigated by mixing the reagents in the solid state. A mechanical grinding of solid $(NH_4)_2[MS_4]$ with pip (Eq. (2)) in a mortar and pestle afforded the new $(pipH)_2[MS_4]$ title compounds. The presence of a monoprotonated organic cation in the product can be readily evidenced by a comparison of the infrared spectra of the solid state reaction products with those of the previously reported $(pipH_2)[MS_4]$ compounds. The IR spectrum of $(pipH)_2[WS_4]$ exhibits two N–H vibrations for the free and protonated amine functionalities (Fig. 1). The sharp signal at 3227 cm^{-1} can be assigned to the N–H vibration of the free amine, while the doublet at around 3000 cm^{-1} can account for the vibration of the protonated amine $(N–H)^+$. In contrast, the IR spectrum of $(pipH_2)[WS_4]$ in which both amine N atoms are protonated, shows a single strong and broad signal centered around 3000 cm^{-1} assignable to the vibrations of the identical $(>N–H_2)^+$ groups. The presence of a free as well as a protonated amine group in the Mo compound **2** can be similarly inferred from its infrared spectrum (Supplementary Fig. 1). In order to prepare suitable crystals of **1** and **2** for structure determination, the reaction conditions were optimized which involves the use of excess pip during grinding followed by recrystallization from water. The products thus obtained, analyzed satisfactorily for new organic $[MS_4]^{2-}$ compounds containing $(pipH)^+$ and $[MS_4]^{2-}$ in a 2:1 mole ratio.

$$(NH_4)_2[MS_4] + pip \xrightarrow{H_2O} (pipH_2)[MS_4] + 2NH_4OH \quad (1)$$

$$(NH_4)_2[MS_4] + 2pip \xrightarrow{grinding} (pipH)_2[MS_4] + 2NH_3 \quad (2)$$

Compounds **1** and **2** which were crystallized from a strongly alkaline medium are not stable in acidic medium and are decomposed to insoluble metal sulfide products. However, on reaction with an aqueous solution of $[Ni(en)_3]Cl_2$ both compounds are converted quantitatively into the insoluble $[Ni(en)_3][MS_4]$ [25,36]. The electronic spectra of the colored compounds **1** and **2** exhibit signals which can be assigned to the intra-ligand charge transitions of the $[MS_4]^{2-}$ moiety and the observed values are in very good agreement with the reported data for $[MS_4]^{2-}$ chromophores [1,26,27].

The title compounds **1** and **2** exhibit several signals in their mid-infrared spectra above 500 cm^{-1} all of which originate from the organic cation, while the M–S vibrations of the $[MS_4]^{2-}$ moiety are observed at lower energies below 500 cm^{-1}. The isotypic $(pipH)_2[MS_4]$ compounds exhibit IR spectra which are identical in terms of their profile as well as number of signals. The only difference is in terms of the W–S vibrations which occur at slightly lower energies as compared to the corresponding isostructural Mo compounds. A comparison of the infrared spectra of both compounds **1** and **2** with those of $(pipH_2)[MS_4]$ reveals that all these spectra are very similar excepting for an additional band assignable for the N–H group of unprotonated N observed in **1** and **2**. The several signals observed above 500 cm^{-1} in the title compounds **1** and **2** can be assigned for the vibrations of the organic cations. For the free tetrahedral $[MS_4]^{2-}$ anion four characteristic vibrations $\upsilon_1(A_1)$, $\upsilon_2(E)$, $\upsilon_3(F_2)$ and $\upsilon_4(F_2)$ are expected. All four bands are Raman active while only υ_3 and υ_4 are IR active. When the tetrahedron is distorted the symmetry is reduced and as a result the symmetric vibration $\upsilon_1(A_1)$ appears in the infrared spectrum at 481 cm^{-1} as a signal of medium intensity and an intense signal for the triply degenerate $\upsilon_3(F_2)$ asymmetric stretching M–S vibration at 465 cm^{-1}. The assignments of these vibrations are in agreement with the literature reports (26, 27, 35–38). The distortion of the tetrahedron is also evident from the appearance of an additional signal at 445 cm^{-1}. The Raman spectra of both the compounds exhibit intense signals for the vibrations of the free and protonated N–H groups as well as the vibrations of the $[MS_4]^{2-}$ moiety (Supplementary Fig. 2). The observed Raman spectral data for the vibrations of the $[MS_4]^{2-}$ unit are in the expected range and add credence to the infrared data. The Mo compound **2** exhibits a similar behavior with the appearance of the $\upsilon_1(A_1)$ vibration in its infrared spectrum as well as additional signals and its IR and Raman spectra can be similarly explained [35–38].

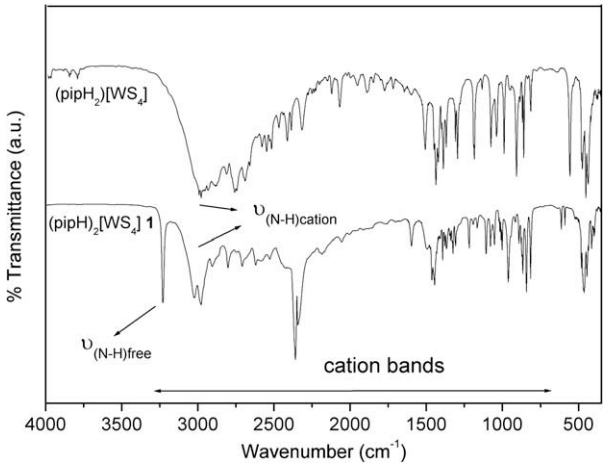

Fig. 1. Infrared spectra of $(pipH_2)[WS_4]$ (top) and $(pipH)_2[WS_4]$ **1** (bottom).

3.2. Description of crystal structures of $(pipH)_2[MS_4]$ (M = W **1**; M = Mo **2**)

The title compounds **1** and **2** are isostructural and crystallize in the centrosymmetric triclinic space group $P\bar{1}$. It is interesting to note that the related isostructural compounds $(pipH_2)[MS_4]$ containing the diprotonated $(pipH_2)^{2+}$ dication crystallize in the monoclinic space group $P2_1/c$ [26,27]. The crystal structures **1** and **2** consist of a tetrahedral $[MS_4]^{2-}$ dianion (M = W **1**; M = Mo **2**), two crystallographically independent piperazin-1-ium cations, all of which are located in general positions (Fig. 2). The monoprotonated cyclic organic ammonium cations adopt a chair confirma-

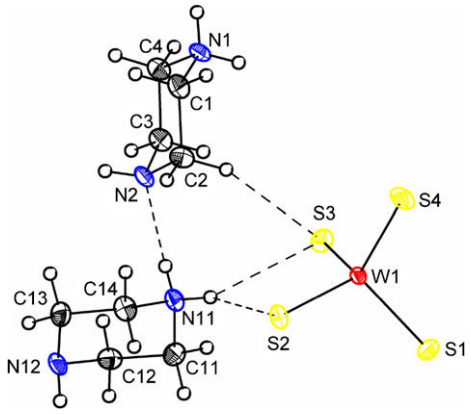

Fig. 2. The crystal structure of $(pipH)_2[WS_4]$ **1** showing the atom-labeling scheme. Displacement ellipsoids are drawn at the 50% probability level except for the H atoms, which are shown as circles of arbitrary radius. Intramolecular H-bonding is shown as broken lines. *Colour code:* C, black; N, blue; W, red; S, yellow. For the structure of the isostructural Mo compound **2**, see Supplementary data. (For interpretation of the references to colour in this figure legend, the reader is referred to the web version of this article.)

tion. In each cation, two of the C–N bond distances (Table 2) associated with the protonated N atoms (N1–C1 = 1.483(7) and N1–C4 = 1.499(6) Å in **1**) are elongated compared to the other two C–N distances made by the free N atom (N2–C2 = 1.466(6) and N2–C3 = 1.461(7) Å in **1**). A similar feature is observed for the C–N bond lengths of the cations in compound **2** (Table 3). This observation can explain the protonation of one of the amine groups of the cyclic diamine in both compounds. In compound **1** the WS_4 tetrahedron is slightly distorted as indicated by the S–W–S bond angles ranging between 108.82(5) and 110.41(5)° (Table 2). The W–S distances vary from 2.1789(7) to 2.2131(7) Å with a mean W–S bond length of 2.1915 Å. In the isostructural $[MoS_4]^{2-}$ compound the Mo–S bonds vary from 2.1734(12) to 2.2115(12) Å with a mean Mo–S bond length of 2.1908 Å (Table 3). The difference Δ between the longest and shortest M–S bond distances is 0.0342 and 0.0368 Å for compounds **1** and **2**, respectively. These Δ values are comparable with the reported Δ value of 0.0385 and 0.0431 Å, respectively, for $(pipH_2)[WS_4]$ and $(pipH_2)[MoS_4]$. Based on an analysis of such Δ values of several $[WS_4]^{2-}$ and $[MoS_4]^{2-}$ compounds, as a structural criterion, we demonstrated that for compounds with Δ larger than 0.033 Å the distortion induces a split M–S vibration in the infrared spectrum [35–38] as observed in the IR spectra of compounds **1** and **2**.

In compound **1**, three of the observed W–S distances (W1–S3, W1–S1 and W1–S4) are shorter than the mean W–S distance of 2.1915 Å indicating a distorted WS_4 tetrahedron. In compound **2** a similar distribution of one long and three short Mo–S bonds is observed. In the related $(pipH_2)[MS_4]$ compounds, a distribution of two short and two long M–S bonds were explained based on the strength and number of hydrogen bonding interactions between the cations and anions. Likewise, the distinct M–S bond lengths in **1** and **2** can be attributed to the several weak hydrogen bonding interactions observed among the $[MS_4]^{2-}$ anions, and the $[pipH]^+$ organic cations. A scrutiny of the structure of **1** reveals a total of 18 weak H-bonding interactions comprising of six N–H···S, two N–H···N and 10 C–H···S contacts the details of which are summarized in Table 4. Thus each $[WS_4]^{2-}$ ion is linked to 10 different piperazin-1-ium cations (Supplementary Fig. 3) with the aid of six N–H···S and 10 C–H···S interactions. One unique $(pipH)^+$ cation (N1, N2) is hydrogen bonded to four different tetrasulfidotungstate anions via three N–H···S and four C–H···S bonds and is further linked to two different cations with the aid of an intramolecular (N11–H5N···N2) and an intermolecular N–H···N interaction. Cation pairs are formed as a result of the intramolecular N–H···N interaction, and the pairs of cations thus formed are extended by the intermolecular N1–H2N···N12 bond into a one-dimensional chain of cations (Fig. 3). The second unique cation is hydrogen bonded to six $[WS_4]^{2-}$ anions and to two different cations with the aid of three varieties of interactions (Supplementary Fig. 4). As a result of H-bonding, a three-dimensional network of H-bonds is formed (see Fig. 4). A detailed analysis of the several H-bonds reveals that the S2 atom which makes the longest W–S distance is involved in two very short N–H···S bonds (N1–H1N···S2 and N11–H4N···S2) at 2.486 and 2.471 Å accounting for its elongation. The isotypic Mo compound **2** exhibits an identical H-bonding behavior (Supplementary Figs. 5–8) and the geometric parameters of its H-bonding interactions are listed in Supplementary Table 1.

Table 2
Selected bond lengths and bond angle (Å, °) for $(pipH)_2[WS_4]$ **1**.

W(1)–S(3)	2.1789(12)	W(1)–S(4)	2.1911(14)
W(1)–S(1)	2.1828(12)	W(1)–S(2)	2.2131(13)
S(3)–W(1)–S(1)	108.94(5)	S(3)–W(1)–S(2)	109.12(5)
S(3)–W(1)–S(4)	110.41(5)	S(1)–W(1)–S(2)	108.82(5)
S(1)–W(1)–S(4)	109.57(6)	S(4)–W(1)–S(2)	109.96(5)
N(1)–C(1)	1.483(7)	N(11)–C(11)	1.487(7)
N(1)–C(4)	1.499(6)	N(11)–C(14)	1.496(6)
C(1)–C(2)	1.522(7)	C(11)–C(12)	1.509(8)
C(2)–N(2)	1.466(6)	C(12)–N(12)	1.468(7)
N(2)–C(3)	1.461(7)	N(12)–C(13)	1.463(7)
C(3)–C(4)	1.514(7)	C(13)–C(14)	1.516(8)
C(1)–N(1)–C(4)	110.5(4)	C(11)–N(11)–C(14)	111.1(4)
N(1)–C(1)–C(2)	108.7(4)	N(11)–C(11)–C(12)	108.9(4)
N(2)–C(2)–C(1)	112.7(4)	N(12)–C(12)–C(11)	113.6(4)
C(3)–N(2)–C(2)	111.4(4)	C(13)–N(12)–C(12)	111.8(4)
N(2)–C(3)–C(4)	113.4(4)	N(12)–C(13)–C(14)	113.8(4)
N(1)–C(4)–C(3)	109.4(4)	N(11)–C(14)–C(13)	108.8(4)

Table 3
Selected bond lengths and bond angle (Å, °) for $(pipH)_2[MoS_4]$ **2**.

Mo(1)–S(3)	2.1734(7)	Mo(1)–S(4)	2.1825(7)
Mo(1)–S(1)	2.1786(7)	Mo(1)–S(2)	2.2115(7)
S(3)–Mo(1)–S(1)	108.84(3)	S(3)–Mo(1)–S(2)	109.12(3)
S(3)–Mo(1)–S(4)	110.39(3)	S(1)–Mo(1)–S(2)	108.86(3)
S(1)–Mo(1)–S(4)	109.61(3)	S(4)–Mo(1)–S(2)	110.00(3)
N(1)–C(1)	1.488(3)	N(11)–C(11)	1.489(3)
N(1)–C(4)	1.490(3)	N(11)–C(14)	1.493(3)
C(1)–C(2)	1.517(3)	C(11)–C(12)	1.512(3)
C(2)–N(2)	1.462(3)	C(12)–N(12)	1.474(3)
N(2)–C(3)	1.467(3)	N(12)–C(13)	1.471(3)
C(3)–C(4)	1.517(3)	C(13)–C(14)	1.504(4)
C(1)–N(1)–C(4)	111.19(19)	C(11)–N(11)–C(14)	111.03(19)
N(1)–C(1)–C(2)	109.01(19)	N(11)–C(11)–C(12)	108.80(19)
N(2)–C(2)–C(1)	113.2(2)	N(12)–C(12)–C(11)	114.2(2)
C(2)–N(2)–C(3)	111.32(19)	C(13)–N(12)–C(12)	111.03(19)
N(2)–C(3)–C(4)	113.8(2)	N(12)–C(13)–C(14)	114.0(2)
N(1)–C(4)–C(3)	109.1(2)	N(11)–C(14)–C(13)	109.38(19)

Table 4
Hydrogen bonding geometry (Å, °) for $(pipH)_2[WS_4]$ **1**.

D–H···A	D(H··A)	d(D··A)	<DHA	Symmetry code
N1–H1N···S1	2.828	3.373	123	$1+x,1+y,z$
N1–H1N···S2	2.486	3.275	153	$1+x,1+y,z$
N1–H2N···N12	2.012	2.859	168	$-1+x,y,z$
N2–H3N···S1	2.837	3.494	134	$x,1+y,z$
N11–H4N···S2	2.471	3.2523	151	x,y,z
N11–H4N···S3	2.861	3.4243	125	x,y,z
N11–H5N···N2	2.010	2.851	166	x,y,z
N12–H6N···S3	2.760	3.446	138	$-1+x,y,z$
C2–H2B···S3	2.825	3.724	153	x,y,z
C4–H4B···S2	2.812	3.629	141	$1-x,1-y,1-z$
C12–H12A···S1	2.779	3.6627	150	$x,1+y,z$
C14–H14A···S4	2.842	3.759	156	$1-x,1-y,1-z$
C3–H3B···S4	2.974	3.928	165	$1-x,1-y,1-z$
C4–H4A···S4	2.884	3.754	149	$x,1+y,z$
C11–H11B···S1	2.929	3.691	135	$1-x,1-y,-z$
C11–H11B···S3	2.942	3.748	140	$1-x,1-y,-z$
C13–H13A···S2	2.971	3.951	178.	$2-x,1-y,1-z$
C14–H14B···S4	2.910	3.803	152	$-1+x,y,z$

3.3. Thermal studies

All the observed thermal events for compounds **1** and **2** as well as the previously reported compounds $(pipH_2)[MS_4]$ containing the diprotonated piperazinediium cation are endothermic and occur below 350 °C. The W compound **1** is thermally more stable as compared to its Mo analogue **2**. An elemental analysis of the residue of all four compounds at 350 °C indicates the presence of considerable amounts of C and N (Table 5). Electron microscopic investigations reveal a porous morphology for the residues and for all the compounds the metal:sulfur ratio of the residue is very close to 1:2. It is well documented that the ammonium salts of the group VI tetrasulfidometalates decompose in two steps resulting in the formation of group VI metal disulfide [52]. The first endothermic

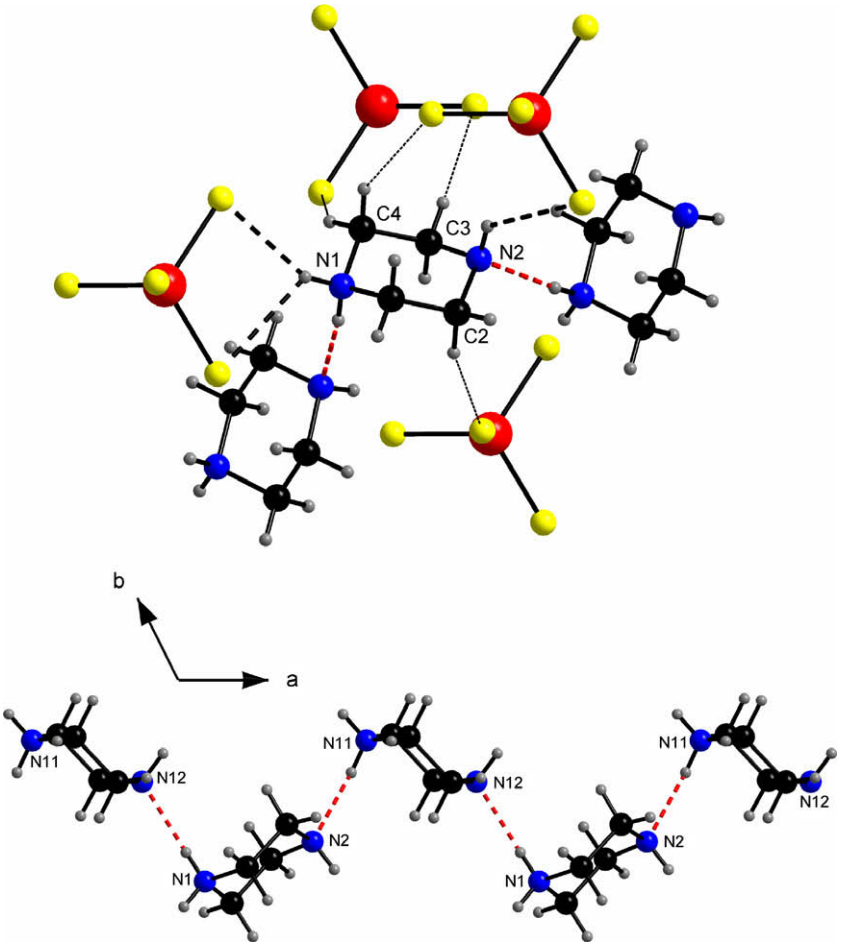

Fig. 3. H-bonding surroundings of one of the unique piperazin-1-ium (N1, N2) cation showing the three varieties of H-bonding interactions (top). The intra and intermolecular N–H···N interactions result in the formation of a one-dimensional H-bonded network of cations in the *ab* crystallographic plane. *Colour code:* C, black; H, medium grey; N, blue; W, red; S, yellow. (For interpretation of the references to colour in this figure legend, the reader is referred to the web version of this article.)

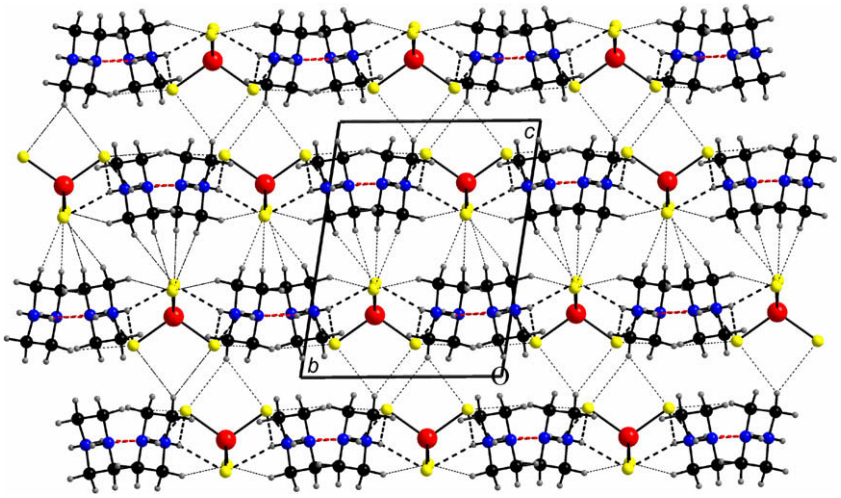

Fig. 4. A view along a axis of the crystallographic packing in compound **1** showing the intricate H-bonded network. H-bonds are shown as broken lines. *Colour code:* C, black; H, medium grey; N, blue; W, red; S, yellow. (For interpretation of the references to colour in this figure legend, the reader is referred to the web version of this article.)

step results in the formation of the amorphous trisulfide accompanied by loss of ammonia and H_2S. In the second step the MS_3 decomposes exothermically above 350 °C into MS_2 losing elemental S. In contrast, organic ammonium $[MS_4]^{2-}$ compounds decompose endothermically at lower temperatures and the decomposition processes are very complex involving structural phase transitions as well as emission of different organic fragments like disulfides and amines [53–55].

The thermal profile of compound **1** (Fig. 5) exhibits two closely related endothermic events centered at 227 and 245 °C as opposed

Table 5
Analytical data of residue at 350 °C.

Compound	C (wt%)	H (wt%)	N (wt%)	S (wt%)	M (wt%)	Composition
$(pipH)_2[WS_4]$ **1**	5.63	0.43	2.52	24.1	67.32	$WS_2C_{1.2}N_{0.5}H_{1.2}$
$(pipH)_2[MoS_4]$ **2**	9.22	0.55	4.18	33.57	52.48	$MoS_{1.9}C_{1.4}N_{0.5}H$
$(pipH_2)[WS_4]$	6.35	0.57	3.02	24.52	65.54	$WS_{2.1}C_{1.4}N_{0.6}H_{1.5}$
$(pipH_2)[MoS_4]$	9.64	0.65	4.32	35.285	50.08	$MoS_{2.1}C_{1.5}N_{0.5}H_{1.2}$

to a single endothermic event for $(pipH_2)[WS_4]$ which shows a single endothermic peak at 290 °C (Supplementary Fig. 9). The observed mass loss of 13.7% is almost twice that expected for the loss of only H_2S, indicating the complex nature of the process. Although the exact nature of thermal event cannot be commented upon in the absence of the mass spectral data of the emitted fragment, it is noted that the TG curve shows a steep drop indicating that the removal of the first fragment leads to further decomposition of **1**. The observed weight loss of 43.5% is lower than the calculated value of 49.4% for the loss of 2 m of pip, H_2S and S. In accordance with this, the observed residue of 56.5% is more than that expected for the formation of WS_2. The analytical data of the residue indicates the composition as $WS_2C_{1.2}N_{0.5}H_{1.2}$.

The DTA curve of $(pipH)_2[MoS_4]$ **2** (Fig. 6) exhibits endothermic events at 165 and 214 °C, respectively, and is very similar to that of $(pipH_2)[MoS_4]$ (see Supplementary Fig. 10). The observed first mass loss is 9.8% is more than the expected value for the removal of only H_2S. The total mass loss of 51.6% till 350 °C is also lower than the expected value of 59.83% for the loss of 2 mol of pip, H_2S and S leading to the formation of MoS_2 indicating incomplete removal of the volatile organic part. This is also evidenced by the presence of C and N in the residue. It is interesting to note that the composition of the residues obtained by the thermal decomposition of the carbon rich starting compounds $(pipH)_2[WS_4]$ **1** and $(pipH)_2[MoS_4]$

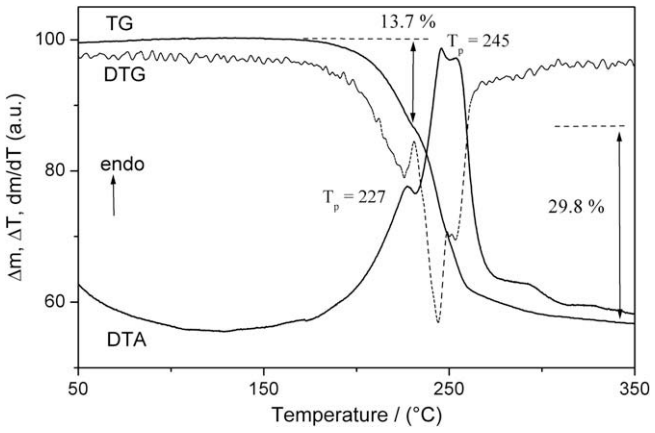

Fig. 5. TG-DTA thermogram of compound **1**.

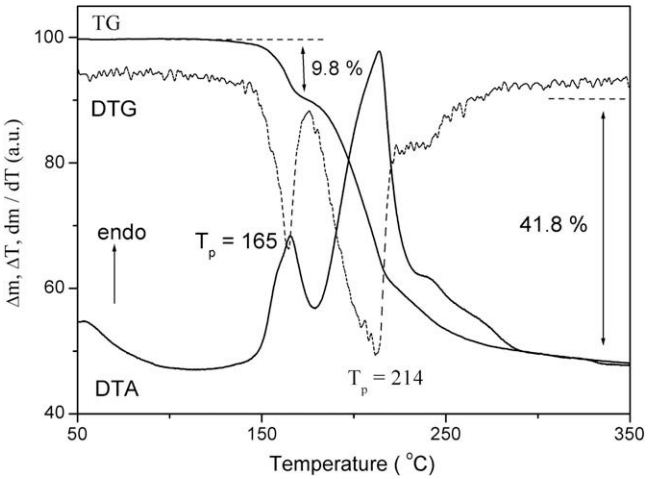

Fig. 6. TG-DTA thermogram of compound **2**.

2 as well as the $(pipH_2)[MS_4]$ compounds which contain the diprotonated piperazine cation are very nearly the same. The results clearly indicate that the carbon content of the precursor tetrasulfidometalates influences the starting decomposition temperature but it does not affect the final carbon content suggesting that the decomposition path for the tetrasulfidometalates containing piperazine cations is very similar and it does not proceed by the formation of MS_3. The formation of the trisulfide as an intermediate is a well documented thermal event for $(NH_4)_2MS_4$.

3.4. Comparative study of tetrasulfidometalates containing piperazine based cations

In addition to the title compounds **1** and **2** described in this work, three more compounds namely $(pipH_2)[WS_4]$, $(pipH_2)[MoS_4]$ and $(2\text{-pipH-1-EtNH}_3)[MoS_4]\cdot\frac{1}{2}H_2O$ (2-pipH-1-EtNH$_3$ = 4-(2-ammonioethyl)piperazin-1-ium) are known. A comparative study of these five compounds (Table 6) reveals certain interesting features. All the compounds which crystallize in centrosymmetric space groups exhibit a very long metal–sulfur bond distance above 2.2005 Å accompanied by Δ values greater than 3 pm and exhibit several weak hydrogen bonding interaction between the organic cation and the $[MS_4]^{2-}$ anion. All compounds including $(pipH_2)[MS_4]$ exhibit N–H···S and C–H···S interactions while the title compounds are additionally involved in N–H···N interactions resulting in the formation of a H-bonded chain of cations. The observed N–H···N interactions in **1** and **2** can be attributed as a possible explanation for the formation of these compounds in the solid state reaction. The hemihydrate $(2\text{-pipH-1-EtNH}_3)[MoS_4]\cdot\frac{1}{2}H_2O$ exhibits four varieties of H-bonding interactions. All compounds decompose endothermically resulting in the formation of residues which contain metal:sulfur in a 1:2 ratio with considerable amounts of C and N.

Table 6
Comparative study of the $[MS_4]^{2-}$ compounds containing organic cations based on piperazine.

Compound	Space group	M–S (long) (Å)	Δ (Å)	H-bonding	Composition of residue[a]	Reference
$(pipH)_2[WS_4]$ **1**	$P\bar{1}$	2.2131	0.0342	N–H···S, C–H···S, N–H···N	$WS_2C_{1.2}N_{0.5}H_{1.2}$	this work
$(pipH)_2[MoS_4]$ **2**	$P\bar{1}$	2.2115	0.0381	N–H···S, C–H···S, N–H···N	$MoS_{1.9}C_{1.4}N_{0.5}H$	this work
$(pipH_2)[WS_4]$	$P2_1/c$	2.2147	0.0385	N–H···S, C–H···S,	$WS_{2.1}C_{1.4}N_{0.6}H_{1.5}$	26
$(pipH_2)[MoS_4]$	$P2_1/c$	2.2114	0.0431	N–H···S, C–H···S,	$MoS_{2.1}C_{1.5}N_{0.5}H_{1.2}$	27
$(2\text{-pipH-1-EtNH}_3)[MoS_4]\cdot\frac{1}{2}H_2O$	$C2/c$	2.2005	0.0302	N–H···S, C–H···S, N–H···O, O–H···S	$MoS_{1.7}C_{2.4}N_{0.7}$[b]	38

Abbreviations: pipH, piperazin-1-ium; $pipH_2$, piperazinediium; 2-pipH-1-EtNH$_3$, 4-(2-ammonioethyl)piperazin-1-ium.
[a] Residue obtained at 350 °C.
[b] Residue obtained at 600 °C.

4. Conclusions

In the present report, we have described a solid state method for the preparation of two new organic tetrasulfidometalates **1** and **2** containing the monoprotonated piperazin-1-ium cation. The title compounds constitute two new examples to the growing list of structurally characterized organic tetrasulfidometalates. The isostructural compounds exhibit three varieties of weak H-bonding interactions between the organic cations and tetrasulfidometalate anion and decompose endothermically resulting in the formation of carbon containing metal sulfide residues.

Acknowledgements

B.R.S. and W.B. acknowledge the financial support by the Indian National Science Academy (INSA), New Delhi, and the Deutsche Forschungsgemainschaft.

Appendix A. Supplementary data

CCDC 715142 and 715143 contain the supplementary crystallographic data for the structures of compounds **1** and **2**, respectively. These data can be obtained free of charge via http://www.ccdc.cam.ac.uk/conts/retrieving.html, or from the Cambridge Crystallographic Data Centre, 12 Union Road, Cambridge CB2 1EZ, UK; fax: (+44) 1223-336-033; or e-mail: deposit@ccdc.cam.ac.uk. Supplementary data associated with this article can be found, in the online version, at doi:10.1016/j.poly.2009.02.034.

References

[1] A. Müller, E. Diemann, R. Jostes, H. Bogge, Angew. Chem., Int. Ed. Engl. 20 (1981) 934. and references therein.
[2] T. Shibhahara, Coord. Chem. Rev. 123 (1993) 73.
[3] D. Coucouvanis, Adv. Inorg. Chem. 45 (1998) 1.
[4] S.H. Laurie, Eur. J. Inorg. Chem. (2000) 2443.
[5] G.J. Brewer, Drug Discovery Today 10 (2005) 1103.
[6] D.E. Schwarz, T.B. Rauchfuss, S.R. Wilson, Inorg. Chem. 42 (2003) 2410.
[7] T.B. Rauchfuss, Inorg. Chem. 43 (2004) 14.
[8] G. Alonso, J. Espino, G. Berhault, L. Alvarez, J.L. Rico, Appl. Catal. A 266 (2004) 29.
[9] M. Poisot, W. Bensch, S. Fuentes, C. Ornelas, G. Alonso, Catal. Lett. 117 (2007) 43.
[10] S.E. Skrabalak, K.E. Suslick, J. Am. Chem. Soc. 127 (2005) 9990.
[11] M. Polyakov, S. Indris, S. Schwamborn, A. Mazheika, M. Poisot, L. Kienle, W. Bensch, M. Muhler, W. Grünert, J. Catal. 260 (2008) 236.
[12] M. Polyakov, M.W.E. van den Berg, T. Hanft, M. Poisot, W. Bensch, M. Muhler, W. Grünert, J. Catal. 256 (2008) 126.
[13] M. Polyakov, M. Poisot, W. Bensch, M. Muhler, W. Grünert, J. Catal. 256 (2008) 137.
[14] H.J. Jakobsen, A.R. Hove, H. Bildsøe, J. Skibsted, M. Brorson, Chem. Commun. 1629 (2007).
[15] M.R. Hansen, M. Brorson, H. Bildsøe, J. Skibsted, H.J. Jakobsen, J. Magn. Reson. 190 (2008) 316.
[16] H.J. Jakobsen, H. Bildsoe, J. Skibsted, M.R. Hansen, M. Brorson, B.R. Srinivasan, W. Bensch, Inorg Chem 48 (2009), <http://dx.doi.org/10.1021/ic8023937>.
[17] C.J. Crossland, I.R. Evans, J.S.O. Evans, Dalton Trans. (2008) 1597.
[18] J. Ellermeier, W. Bensch, Z. Naturforsch. 56b (2001) 611.
[19] J. Ellermeier, W. Bensch, Monatsh. Chem. 133 (2002) 945.
[20] B.R. Srinivasan, S.N. Dhuri, A.R. Naik, Tetrahedron Lett. 45 (2004) 2247.
[21] B.R. Srinivasan, J. Chem. Sci. 116 (2004) 251.
[22] B.R. Srinivasan, B.K. Vernekar, K. Nagarajan, Indian J. Chem. 40A (2001) 563.
[23] B.R. Srinivasan, S.N. Dhuri, C. Näther, W. Bensch, Acta Crystallogr. E58 (2002) m622.
[24] B.R. Srinivasan, S.N. Dhuri, C. Näther, W. Bensch, Acta Crystallogr. C59 (2003) m124.
[25] B.R. Srinivasan, S.N. Dhuri, C. Näther, W. Bensch, Inorg. Chim. Acta 358 (2005) 279.
[26] B.R. Srinivasan, S.N. Dhuri, M. Poisot, C. Näther, W. Bensch, Z. Anorg. Allg. Chem. 631 (2005) 1087.
[27] B.R. Srinivasan, S.N. Dhuri, M. Poisot, C. Näther, W. Bensch, Z. Naturforsch. 59b (2004) 1083.
[28] J.W. McDonald, G.D. Friesen, L.D. Rosenhein, W.E. Newton, Inorg. Chim. Acta 72 (1983) 205.
[29] G. Alonso, G. Berhault, R.R. Chianelli, Inorg. Chim. Acta 316 (2001) 105.
[30] B.R. Srinivasan, S.N. Dhuri, C. Näther, W. Bensch, Acta Crystallogr. E59 (2003) m681.
[31] B.R. Srinivasan, M. Poisot, C. Näther, W. Bensch, Acta Crystallogr. E60 (2004) i136.
[32] B.R. Srinivasan, C. Näther, W. Bensch, Acta Crystallogr. E61 (2005) m2454.
[33] B.R. Srinivasan, C. Näther, A.R. Naik, W. Bensch, Acta Crystallogr. E62 (2006) m1635.
[34] B.R. Srinivasan, C. Näther, W. Bensch, Acta Crystallogr. C62 (2006) m98.
[35] B.R. Srinivasan, C. Näther, S.N. Dhuri, W. Bensch, Monatsh. Chem. 137 (2006) 397.
[36] B.R. Srinivasan, C. Näther, S.N. Dhuri, W. Bensch, Polyhedron 25 (2006) 3269.
[37] B.R. Srinivasan, A.R. Naik, C. Näther, W. Bensch, Z. Anorg. Allg. Chem. 633 (2007) 582.
[38] B.R. Srinivasan, S.N. Dhuri, A.R. Naik, C. Näther, W. Bensch, Polyhedron 27 (2008) 25.
[39] B.R. Srinivasan, A.R. Naik, C. Näther, W. Bensch, Acta Crystallogr. E62 (2006) m3491.
[40] B.R. Srinivasan, A.R. Naik, C. Näther, W. Bensch, Acta Crystallogr. C63 (2007) m81.
[41] B.R. Srinivasan, C. Näther, W. Bensch, Acta Crystallogr. E63 (2007) i167.
[42] B.R. Srinivasan, S.V. Girkar, P. Raghavaiah, Acta Crystallogr. E63 (2007) m2737.
[43] B.R. Srinivasan, S.V. Girkar, P. Raghavaiah, Acta Crystallogr. E63 (2007) m3100.
[44] B.R. Srinivasan, C. Näther, A.R. Naik, W. Bensch, Acta Crystallogr. E64 (2008) m66.
[45] B.R. Srinivasan, C. Näther, W. Bensch, Acta Crystallogr. E64 (2008) m296.
[46] M. Poisot, C. Näther, W. Bensch, Z. Naturforsch. 61b (2006) 1061.
[47] M. Poisot, C. Näther, W. Bensch, Z. Naturforsch. 62b (2007) 209.
[48] M. Poisot, C. Näther, W. Bensch, Acta Crystallogr. E62 (2006) m1326.
[49] U. Siemeling, F. Bretthauer, C. Bruhn, Z. Anorg. Allg. Chem. 632 (2006) 1027.
[50] M.G. Kanatzidis, D. Coucouvanis, Acta Crystallogr. C39 (1983) 835.
[51] G.M. Sheldrick, Acta Crystallogr. A64 (2008) 112.
[52] T.P. Prasad, E. Diemann, A. Müller, J. Inorg. Nucl. Chem. 35 (1973) 1895.
[53] B.R. Srinivasan, S.N. Dhuri, C. Näther, W. Bensch, Transition Met. Chem. 32 (2007) 64.
[54] M. Poisot, W. Bensch, S. Fuentus, G. Alonso, Theromochim. Acta 444 (2006) 35.
[55] M. Poisot, W. Bensch, Theromochim. Acta 453 (2007) 42.